Multiscale Contrast Enhancement for Radiographies: Laplacian Pyramid Versus Fast Wavelet Transform

Sabine Dippel*, Martin Stahl, Rafael Wiemker, and Thomas Blaffert

***Abstract*—Contrast enhancement of radiographies based on a multiscale decomposition of the images recently has proven to be a far more versatile and efficient method than regular unsharp-masking techniques, while containing these as a subset. In this paper, we compare the performance of two multiscale-methods, namely the Laplacian Pyramid and the fast wavelet transform (FWT). We find that enhancement based on the FWT suffers from one serious drawback—the introduction of visible artifacts when large structures are enhanced strongly. By contrast, the Laplacian Pyramid allows a smooth enhancement of large structures, such that visible artifacts can be avoided. Only for the enhancement of very small details, for denoising applications or compression of images, the FWT may have some advantages over the Laplacian Pyramid.**

***Index Terms*—Fast wavelet transform, image enhancement, mammography, multiscale methods, radiography.**

I. Introduction

In digital radiography, suitable image processing can help to reconcile some of the problems faced in the display of radiographic images. Radiographs often contain at the same time large contrast variations and important low-contrast details. Suitable postprocessing can help to meet the conflicting requirements of reproducing the low-contrast details without clipping the general gray-value range. A standard technique for the enhancement of small details (i.e., edges) is unsharp masking [1], where the image is split up into two or three frequency channels. The edge image is then amplified and added again to the corresponding low-pass image. In the case where the image is split into three frequency channels, a contrast equalization can be achieved by additionally applying a dynamic range compression to the low-pass image. Clearly, this provides no access to structures of intermediate sizes. Therefore, various multiscale methods have been proposed recently, where the image is split up into a larger number of frequency channels, which can then be processed separately.

In medical image processing, multiscale methods have been used for many purposes, e.g., in the context of segmentation [2], registration [3], noise reduction [4], or compression of images [5]–[7]. Mostly, these applications used wavelet methods for the multiscale decomposition of the signal (for a review of wavelet applications in biomedical signal processing in general, see [8]).

Only within the last decade, multiscale methods have been applied to contrast enhancement of medical images. Two types of multiscale methods have been used in this context: the Laplacian Pyramid [9], [10] and wavelet methods [12]–[15]. We want to stress here that by contrast enhancement we do not mean image enhancement via reduction or suppression of noise, which we will not discuss here, but rather contrast amplification of the structures of interest. Clearly, contrast amplification will amplify noise, too, if no additional steps are taken to prevent this. However, we will not discuss such methods here, but instead focus on methods to enhance details at different scales—be they noise or anatomical structure. For a discussion of methods to prevent too strong amplification of noise, see [10] for the Laplacian Pyramid and [13] for wavelet methods. While enhancement by means of the Laplacian Pyramid was applied to X-ray images in general [9], [10], wavelet-based methods were mainly used in the context of mammography [12]–[14], although there are also some isolated applications to magnetic resonance (MR) and computed tomography (CT) images [12] or chest radiographs [15]. With nonlinear multiscale enhancement based on the Laplacian Pyramid, we obtained very satisfactory results in two clinical trials [10]. There are reasons why one might expect that wavelet-based enhancement could be even more powerful than the Laplacian Pyramid: perfect decomposition due to orthogonality of the wavelet bases, direction sensitivity, and high noise-reduction potential. In this paper, we explore the possibilities of enhancement via the fast wavelet transform (FWT) for radiographs and compare them with results from the Laplacian Pyramid, since no comparison of these different multiscale methods has been performed so far. We restrict ourselves to pyramidal methods of decomposition, since for radiographs, which are usually quite large (up to 3 k $\times$ 3 k pixels), such methods seem to be most appropriate, both for reasons of disc space and computation time. Especially if the multiscale processing is to be integrated in the regular processing chain of a digital radiography system, processing times of more than 10 s are usually unacceptable.

We compare the suitability of these methods for enhancement of radiographs in general, i.e., we are looking for an approach which will be applicable to any kind of radiographic application (skeleton, chest, abdomen, mammography, etc.). Generally, an enhancement algorithm faces the challenge of enhancing the contrast of barely visible details, without distorting the overall image impression by over-amplification of structures which are already clearly visible. The case of mammograms is typical of images which at the same time contain low-contrast structures

Manuscript received January 3, 2000; revised March 1, 2002. The Associate Editor responsible for coordinating the review of this paper and recommending its publication was S. Pizer. *Asterisk indicates corresponding author.*

*S. Dippel was with the Philips Research Laboratories, Division Technical Systems, Röntgenstr. 24-26, 22335 Hamburg, Germany. She is now with the FB Elektro- und Informationstechnik, Fachhochschule Hannover, Postfach 92 02 61, 30441 Hannover, Germany (e-mail: dippel@etech.fh-hannover.de).

M. Stahl is with the Philips Medical Systems, 22335 Hamburg, Germany.

R. Wiemker and T. Blaffert are with the Philips Research Laboratories, Division Technical Systems, 22335 Hamburg, Germany.

Publisher Item Identifier S 0278-0062(02)04689-X.

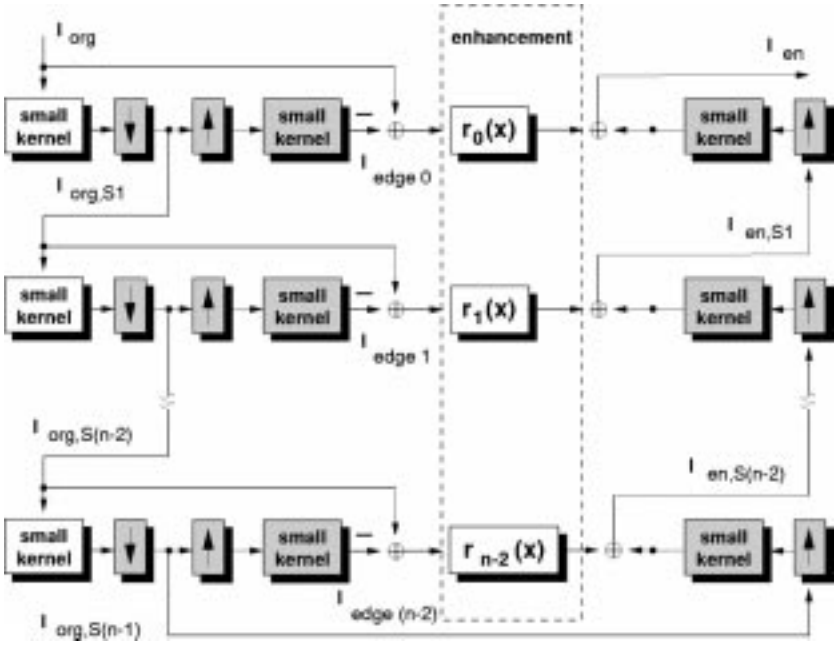

Fig. 1. The Laplacian Pyramid with subband remapping. The $r_i(x)$ in the dashed box "enhancement" denote the remapping functions that may be applied to the bandpass images.

in the breast combined with a very large general gray value variation between background and tissue. Here, essentially any enhancement of the low-contrast structures is welcomed. Some of the results presented in [13], [14] for mammography change the image impression significantly. This would probably be unacceptable for general radiographic applications.

The outline of the paper is as follows. In Section II, we briefly present the Laplacian Pyramid and the FWT.[1] This includes a survey of previous applications of these methods to radiographs. In Section III, we compare the effect of contrast enhancement in the framework of these different decomposition methods and discuss the influence of their properties on the perception of radiographic images. A final discussion of the merits and problematic points of the different methods follows in Section IV.

II. Multiscale Decomposition and Enhancement of Images

A. The Laplacian Pyramid Decomposition Scheme

The Laplacian Pyramid was introduced by Burt and Adelson in the context of compression of images [16]. It has the advantage that the image is only expanded to 4/3 of the original size and that the same (small) filter kernel can be used for all pyramid levels. Fig. 1 schematically shows the algorithm. The image is filtered with a small kernel (we use a binomial 5×5-kernel, which leads to a Laplacian filter for the high-pass images). In each filter step, the previous low-pass image (in the first step, this is the original image) is smoothed by the small kernel and sub-sampled by a factor of two to give the next low-pass image. This new low-pass image is up-sampled again by inserting zeros after each pixel and smoothed once more with the small kernel before it is subtracted from the previous low-pass image. The sequence of low-pass images is termed a Gaussian Pyramid, while the sequence of the subtracted (bandpass) images $I_{\text{edge}\,0}, \ldots, I_{\text{edge}\,(n-2)}$ is termed a Laplacian Pyramid.

For enhancement of images by means of a Laplacian Pyramid decomposition, the bandpass images are mapped by a (usually nonlinear) function. In [9] and [10], nonlinear functions were used and shown to give good results. Vuylsteke and Schoeters [9] used a power law with a linear lower and upper cutoff

$$r(x) = \begin{cases} GM\frac{x}{x_c}\left(\frac{x_c}{M}\right)^p, & \text{for } |x| < x_c \\ GM\frac{x}{|x|}\left(\frac{|x|}{M}\right)^p, & \text{for } x_c \le |x| \ge M, \cdot \\ x & \text{elsewhere} \end{cases} \quad (1)$$

Stahl *et al.* [10] used a power law bounded by linear functions for very small and very large contrast

$$r(x) = \begin{cases} G \cdot x \cdot \left(1 - \frac{|x|}{M}\right)^p + x, & \text{for } |x| \le M \\ x, & \text{elsewhere} \end{cases} . \quad (2)$$

Here, x_c is a lower cutoff value introduced to avoid too strong amplification of noise and M is the upper limit for the nonlinear enhancement. G is a constant gain factor. While Vuylsteke and Schoeters [9] used the same remapping parameters in all subbands, Stahl *et al.* [10] introduced a variation of the gain G in all subbands, as well as other additional features not shown in Fig. 1 to adapt the remapping to the image type at hand. These special features include noise robustness and a density-dependent enhancement. For more detail, see [10].

With these additional features incorporated in the enhancement algorithm, we conducted an observer-preference study at Fulda Municipal Hospital (Fulda, Germany). Results obtained on a large variety of image types showed that by careful selection of the parameters on the different scales improved detail visibility and improved overall contrast and sharpness could be

[1]In the literature, the nomenclature for this is somewhat inconsistent. The algorithm we present here is sometimes termed FWT, sometimes Mallat algorithm, and sometimes pyramid algorithm.

achieved, retaining a balanced image impression while avoiding boosting noise too strongly [10]. A receiver operating characteristic study performed on phantoms and chest images with simulated lesions at the Medical University Hannover (Hannover, Germany) showed a general trend toward better detection for most lesion types [11] for the multiscale processed images, again without affecting the image impression in a negative way. Generally, especially for images showing an overlay of many structures, such as chest, pelvis, lateral images of the spine, etc., the processing was judged to render all these structures more visible.

B. FWT

Wavelets are functions which are generated by the dilation and translation of a single function ψ

$$\psi^{a,b}(t) = |a|^{-1/2}\psi\left(\frac{t-b}{a}\right). \tag{3}$$

(Clearly, this can be generalized for arbitrary dimensions, but for the sake of clarity, we discuss only the one-dimensional case here.) In practical applications, particularly for the discrete wavelet transform, often $a = 2^j$, $j \in \mathbf{Z}$ is chosen for the dilation. The data points define a natural grid for the values of the translation parameter b. A wavelet transform with $a = 2^j$ is termed *dyadic wavelet transform*. The so-called *mother wavelet* ψ has to satisfy the condition $\int dt\,\psi(t) = 0$. (Actually, the condition is one on the Fourier transform of ψ, however, for a wavelet with compact support, this is equivalent to the condition stated here.)

A wavelet transform is now simply the representation of a function f by a superposition of wavelets. In the discrete case, the function can be represented as

$$f = \sum c_{m,n}(f)\psi_{m,n} \tag{4}$$

where $\psi_{m,n}(t) = a_0^{-m/2}\psi\left(a_0^{-m}t - nb_0\right)$. It can be shown that there exist choices for ψ such that the $\psi_{m,n}$ constitute an orthonormal basis of $L^2(\mathbf{R})$. Then, the coefficients $c_{m,n}$ are given by

$$c_{m,n}(f) = \langle \psi_{m,n}, f\rangle = \int dt\,\psi_{m,n}(t)f(t). \tag{5}$$

Such orthonormal bases can be constructed iteratively by a multiresolution analysis, where the signal is approximated on scales of decreasing resolution. This analysis was introduced by Mallat [17], who also pointed out the connection between multiscale decomposition schemes like the Laplacian Pyramid and a multiresolution approximation on the basis of a wavelet decomposition in [18]. While in the Laplacian Pyramid, information in successive levels is correlated (the transform is oversampled by a factor of 4/3), it is possible to achieve an exact separation of details based on an orthogonal wavelet representation, denoted as multiresolution approximation.

In a multiresolution approximation, in addition to the wavelet ψ, a *scaling function* ϕ is defined, which is a smoothing function. The approximation of the function f at resolution $j-1$ (the projection $P_{j-1}f$ of f onto the approximation space V_{j-1}) is then given by

$$P_{j-1}f = P_j f + \sum_{k\in\mathbf{Z}} \langle f, \psi_{j,k}\rangle\,\psi_{j,k} \tag{6}$$

with

$$P_j f = \sum_{k\in\mathbf{Z}} \langle f, \phi_{j,k}\rangle\,\phi_{j,k}. \tag{7}$$

From the orthogonality of the bases $\{\phi_{j,k}; k \in \mathbf{Z}\}$ and $\{\psi_{j,k}; j,k \in \mathbf{Z}\}$, a pyramidal algorithm can be derived, where the approximation of the function f at resolution level m at point n can recursively be calculated by

$$a_m(n) = \langle f, \phi_{m,n}\rangle = \sum_k h_{k-2n}\,\langle f, \phi_{m-1,n}\rangle\,. \tag{8}$$

The detail signal (i.e., the edges at level m) is given by

$$d_m(n) = \langle f, \psi_{m,n}\rangle = \sum_k g_{k-2n}\,\langle f, \psi_{m-1,n}\rangle\,, \tag{9}$$

with $g_k = (-1)^k h_{-k+1}$ and $h_k = \langle \phi, \phi_{-1,k}\rangle$.

However, there are some drawbacks of orthonormal wavelet bases. It can be shown that there are no nontrivial orthonormal linear phase FIR filters with exact reconstruction (the trivial exception is the Haar basis with $h_0 = h_1 = \sqrt{2}$ and $g_0 = -g_1 = \sqrt{2}$, all other $h_n = g_n = 0$). Linear phase (which is desirable, e.g., for the possibility to use reflecting instead of periodic boundary conditions) can be preserved by relaxing the orthonormality requirement and requiring biorthogonality instead [19]. A biorthogonal wavelet basis is simply one where the reconstruction filters $\tilde{h}$ and $\tilde{g}$ may be different from h and g, but fulfill the reconstruction requirement

$$a_{m-1}(l) = \sum_n \left[\tilde{h}_{2n-l}a_m(n) + \tilde{g}_{2n-l}d_m(n)\right] \tag{10}$$

and are related to h and g by

$$\tilde{g}_n = (-1)^n h_{-n+1} \text{ and } g_n = (-1)^n \tilde{h}_{-n+1} \tag{11}$$

with

$$\sum_n h_n \tilde{h}_{n+2k} = \delta_{k,0}. \tag{12}$$

Antonini *et al.* [19] give the corresponding filter coefficients for a number of such biorthogonal wavelet bases and test their performance when applied to image compression. To our knowledge, none of these wavelets has so far been applied to image enhancement. In Section III, we will discuss enhancement results for one of these wavelet types.

The above discussion can be generalized for images, where we then end up with three "detail images"—one which is low-pass filtered in the x direction and high-pass filtered in the y direction (D_m^y), one which is low-pass filtered in the y direction and high-pass filtered in the x direction (D_m^x) and finally one which is high-pass filtered in both directions (D_m^{xy}, often termed "diagonal image"). The structure of the pyramidal decomposition and reconstruction in the two-dimensional case

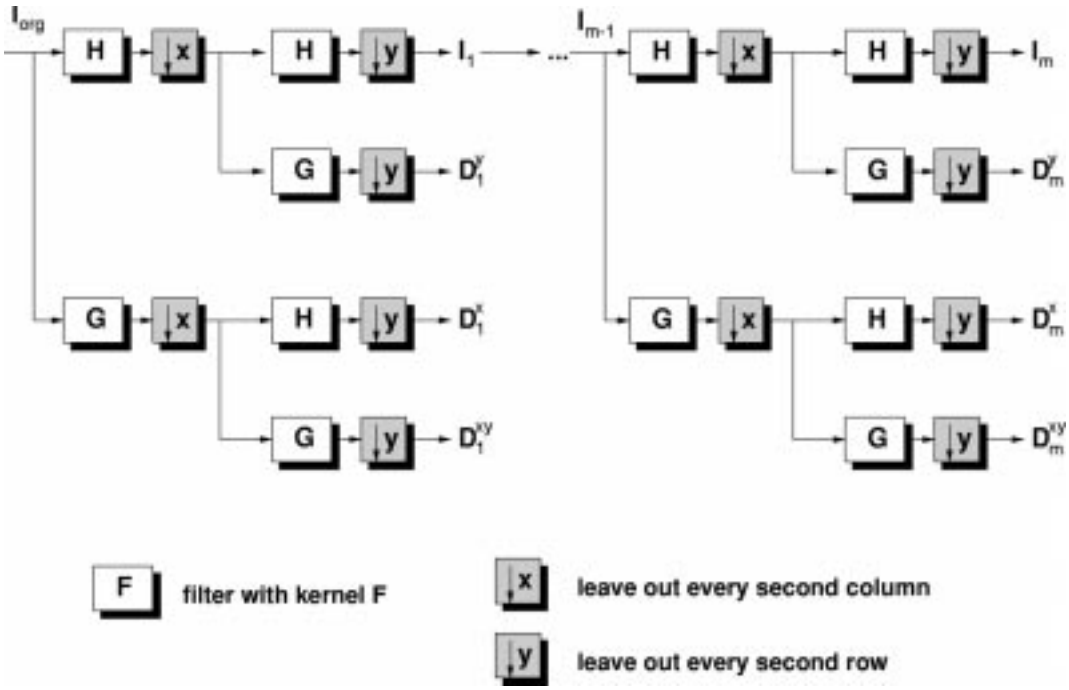

Fig. 2. Filter bank representation of the wavelet decomposition of an image.

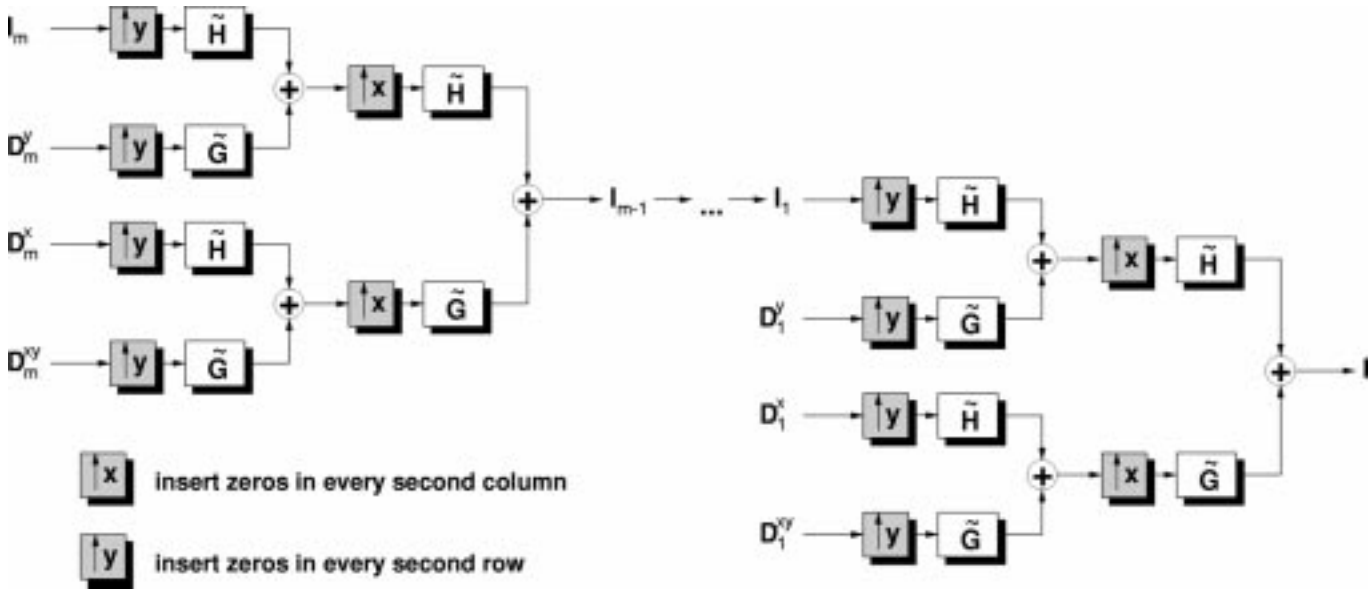

Fig. 3. Filter bank representation of the back transformation corresponding to the decomposition shown in Fig. 2. $\tilde{H}$ and $\tilde{G}$ denote the inverse filters of H and G. Though in the orthonormal case, $\tilde{H} = H$ and $\tilde{G} = G$, in more general cases, e.g., for biorthogonal wavelets as discussed below, they may differ.

is shown in Figs. 2 and 3. The FWT is usually represented as in Fig. 4.

The FWT is not the only type of wavelet transform that may be used—and has been used—for the enhancement of images. Enhancement of medical images by means of a wavelet decomposition was so far mainly performed on images decomposed in a different way than presented above. Laine *et al.* [13], [14] used both a redundant wavelet transform and reconstruction from wavelet maxima. The latter method was also applied to MR and CT images by Lu *et al.* [12]. In the redundant wavelet transform, the scaling of the wavelet is not achieved by subsampling of the image in each step, as in the pyramidal algorithm described above, but rather by a scaling of the filter. Non-orthogonal wavelets can, therefore, be used in the transform. Laine *et al.* [13], [14], e.g., used a Laplacian filter and, thus, in fact performed a decomposition very similar to the Laplacian Pyramid, but without the pyramidal structure. They then used a linear remapping with two different slopes. The results obtained with this enhancement do not alter the general image impression as much as their results with other methods.

Another method of wavelet decomposition, which is especially suitable for image compression and denoising, is the coding of an image by wavelet maxima [20]. There, a regular (redundant) wavelet transform is applied to the image,

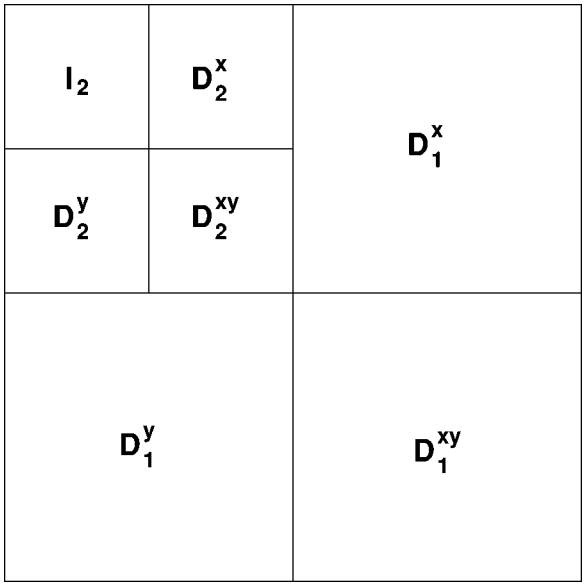

Fig. 4. Represents the way in which a decomposed image is usally stored or presented.

but in a subsequent step only the position and magnitude of the edges (i.e., wavelet maxima) of the detail images are retained. The original image can be reconstructed in an iterative process, which converges to the original image. In the first 20 iteration steps, convergence is quite fast, however, afterwards it slows down considerably. The algorithm is in fact a very good tool for noise reduction. Laine *et al.* performed contrast enhancement on mammograms by applying a constant, but scale-dependent gain on the wavelet maxima (with a lower limit to avoid boosting of noise) [13]. Lu *et al.* did the same for mammograms, MR and CT images, but without the noise robustness feature [12]. The results for mammograms do not look as convincing as with the redundant wavelet transform as far as the general image impression is concerned. Note also that due to the large number of iteration steps needed to get a good approximation of the original image, this method is quite time-consuming.

To our knowledge, none of the wavelet-based enhancement methods described here has been tested in clinical routine so far. In Section III, we will discuss the possibility of image enhancement based on the FWT and compare it with the results obtained by a Laplacian Pyramid. Some properties of the FWT indicate that it might give better results than the Laplacian Pyramid. One would expect that the selective enhancement of structures of a certain size might be possible in an image where the detail information of successive layers is orthogonal and that the isolation of noise might be achieved more effectively in a wavelet framework than in a Laplacian Pyramid.

III. Comparison of the Decomposition Schemes

Obviously, a comparison of the performance of the two decomposition schemes is a difficult task, since there is a variety of possible filters that might be used in the wavelet transform and an even greater variety of possible subband remapping functions. As far as the remapping is concerned, we will, therefore, discuss the effect of a simple linear remapping of the subbands, where the slope of the remapping look-up table (LUT) may vary over the different scales. This should capture the essential effects of a general remapping of the subbands, while at the same time facilitating comparison between different decomposition methods. It also has the advantage that due to the use of constant remapping factors for the subbands, in the case of the FWT the enhancement is the same if remapping is applied to the wavelet coefficients directly or to the reconstructed wavelet channel [this can be seen from the linearity of (10)]. In the case of a nonlinear remapping function, this would not be true.

TABLE I
Filter Coefficients of the Bi-Orthogonal 7–9-Tap Wavelet Used in the Comparison

n	0	±1	±2	±3	±4
$2^{-1/2}h_n$	0.602949	0.266864	-0.078223	-0.016864	0.026749
$2^{-1/2}\tilde{h}_n$	0.557543	0.295636	-0.28772	-0.045636	0

It is beyond the scope of this paper to discuss all wavelet types that might be used for image decomposition and enhancement. Therefore, for the wavelet transform, we restrict ourselves to two different wavelet types: an orthonormal one, namely a Daubechies wavelet and a biorthogonal one introduced in [19], which is quite close to an orthonormal wavelet and showed best results for the compression of images out of the biorthogonal wavelets discussed in [19]. The filter coefficients of this biorthogonal 7–9-tap wavelet from [19] are given in Table I, for the Daubechies wavelets, see, e.g., [21] and [22].

For the comparison, we use two characteristically different images. The first is a posterior-anterior (pa) image of a skull (Fig. 5), since it contains large, low-contrast structures such as the marking of the calotte by vessels, small low-contrast structures, such as the facial structure and the nasal bone and quite sharp edges, such as the skull-background transition and the fillings. In this particular image, there is a very low-contrast occipital fracture (behind the right eye), which is nearly invisible in the original unprocessed image. The second image we use is a mammogram (Fig. 9), since this is the image type used most in previous works on wavelet-based image enhancement. The images were obtained by a Philips PCR 9000 computed radiography system, which already performs pre-ranging of the images.

For the linear enhancement of the skull image, we used the gain values found to be optimal in an observer preference study at Fulda Municipal Hospital for pa-skull images in the case of nonlinear remapping with function (2). It has to be noted here that in addition to the gain G in (2), a global (constant) enhancement factor was applied to all subbands. For the linear enhancement, we, therefore, used the product of the remapping gain G from (2) and this global enhancement factor. These gain values (see figure captions) were used both for remapping of the Laplacian Pyramid decomposition and the wavelet decomposition. For comparison, the corresponding result for nonlinear enhancement of the Laplacian Pyramid decomposition is shown as well. There, however, we did not include the noise-robustness feature used in [10], to facilitate comparison with the linear case.

Fig. 5. Original image of skull.

Fig. 6. Skull processed with Laplacian Pyramid and linear remapping. The gain in the subbands was $g_0 = 1.68$, $g_1 = 1.68$, $g_2 = 1.68$, $g_3 = 2.4$, $g_4 = 2.4$, $g_5 = 2.4$, $g_6 = 2.4$.

It is clear that the selection of the gain values used in the Laplacian Pyramid might introduce a bias toward this decomposition method in the comparison of the two decomposition schemes, since the wavelet decomposition splits up the image differently and the wavelet coefficients are not comparable with the gray values of the Laplacian Pyramid levels. However, tests of many different parametrizations of the wavelet-based enhancement showed that the characteristics we are going to discuss here do not change by using different parameters—either hardly any enhancement is visible, or certain artifacts are visible very well—regardless of the parametrization. We will come back to this later when discussing results of enhancement of synthetic edges.

Figs. 6–8 show the results obtained with the different remapping and decomposition types. The wavelet decomposition was performed with the biorthogonal 7–9-tap wavelet. Obviously, linear and nonlinear enhancement via the Laplacian Pyramid show very similar results as compared to the FWT results. The sharper edges in the linearly enhanced image (Fig. 6) seem to disturb the harmonic image impression a little, but there are no obvious artifacts (e.g., ringing). The image enhanced via the FWT instead gives a distinctly different impression. Apart from the very disturbing artifacts visible near strong edges (e.g., skull-cap/background or fillings), the general image impression is far more "high-pass-like" than in the Laplacian Pyramid enhanced cases. The fine structure seems to come out more clearly, which is best seen by the very good delineation of the fracture, but this renders the image "busier." We will see later that the occurrence of these artifacts is a problem inherent to the wavelet

Fig. 7. Skul processed with Laplacian Pyramid and nonlinear remapping according to (2). Parameters: gain, see Fig. 6, structure boost: $p_0 = 5.0$, $p_1 = 5.0$, $p_2 = 5.0$, $p_3 = 2.0$, $p_4 = 2.0$, $p_5 = 2.0$, $p_6 = 2.0$.

Fig. 8. Skull, processed with wavelet pyramid and linear remapping of subbands. The gain in the subbands was the same as for Fig. 6.

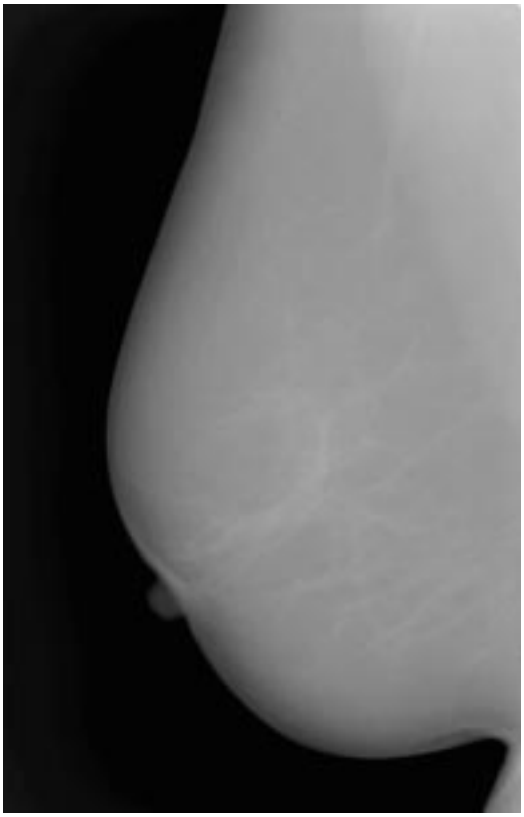

Fig. 9. Mammogram (original image).

transform itself and is not caused by a bad choice of remapping parameters or the type of wavelet.

The question is now whether this effect is observable as well in mammograms, which so far have shown quite promising results when other wavelet-based enhancement methods were used. Figs. 9–11 show the results obtained for the same remapping types as for the skull. However, the parameters used here were the ones which in our clinical study at Fulda Municipal Hospital showed to be optimal for lateral images of the sacrum, which just like the mammograms is characterized by many superposing structures of all sizes and low contrast [23].

Apparently, the problems which occur for the skull images persist in the mammograms. Apart from that, the Laplacian Pyramid enhancement gives very promising results, especially with nonlinear remapping. In fact, the strong ringing artifacts in the FWT-enhanced images arise from a property of the FWT itself. They are not a result of the wavelet-type or remapping parameters used (in fact, as we will see, this wavelet type is least affected by this artifact of the types we have tested).[2]

The fact that the artifacts are inherent in the FWT becomes clear when we regard the step-response of the wavelet- and Laplacian Pyramid-based enhancement. Figs. 13–16 show the response of a wavelet-based and a Laplacian Pyramid-based

[2]The additional strong ringing artifacts at the top and right edges of the mammogram are a result of the (artificial) edges produced by the periodic boundary conditions we used for the wavelet transform (though not for the Laplacian Pyramid). Although for the biorthogonal wavelet used, reflecting boundary conditions are possible, this is not the case for the (nonshift-invariant) orthogonal Daubechies wavelets.

Fig. 10. Mammogram processed with Laplacian Pyramid, but linear remapping. The gain in the subbands was $g_0 = 3.0$, $g_1 = 3.0$, $g_2 = 3.0$, $g_3 = 3.9$, $g_4 = 3.9$, $g_5 = 3.9$, $g_6 = 3.9$.

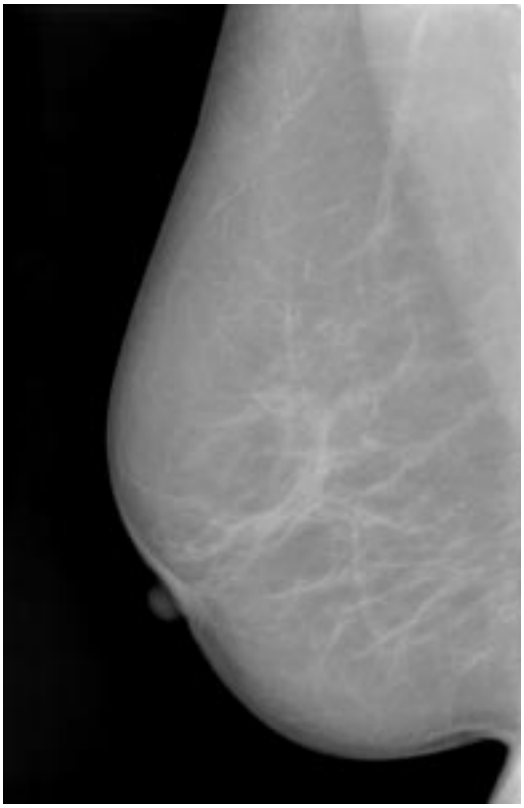

Fig. 11. Mammogram processed with Laplacian Pyramid and nonlinear remapping according to (2). Parameters: gain, see Fig. 10, boost: $p_0 = 2.1$, $p_1 = 2.1$, $p_2 = 2.1$, $p_3 = 1.2$, $p_4 = 1.2$, $p_5 = 1.2$, $p_6 = 1.2$.

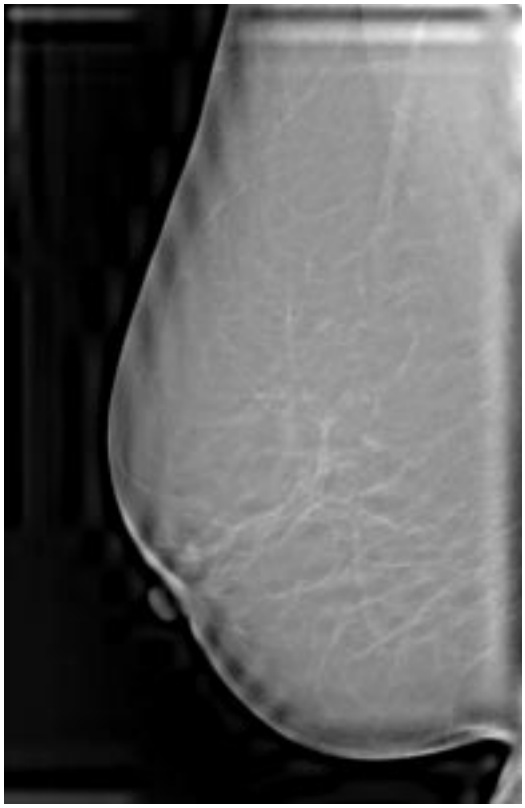

Fig. 12. Mammogram processed with wavelet pyramid and linear remapping of subbands. The gain in the subbands was the same as for Fig. 10.

enhancement to a step-edge, where only one level at a time is mapped by a linear LUT with slope 2. The difference between (all) wavelet types and the Laplacian Pyramid is striking. All wavelets exhibit an additional overshooting at the edge (additional to the inevitable one which in fact is a result of linear enhancement of a bandpass image). It is most severe for the (orthogonal) Daubechies wavelets. Particularly, there is no large difference between the Daubechies wavelets of 4th and 12th order, except for the fact that the 12th order wavelet results in smoother waveforms around the edge. In fact, what we see on the edges is mainly the wavelet itself on this particular scale. In the case of the Daubechies wavelets, the asymmetric response of the wavelets is due to the asymmetry of the wavelet itself. In the case of the biorthogonal wavelet, it arises from the fact that high- and low-pass filter are shifted by one pixel with respect to each other, which is why the asymmetry disappears for lower scales, since then the exact position of the filters with respect to the edge is no longer so important due to the smoothing of the edge.

Figs. 13–15 in fact explain the appearance of Figs. 8 and 12 with respect to their counterparts enhanced via the Laplacian Pyramid. While at high-resolution levels the second overshoot is relatively small compared to the one directly at the edge, its height grows to the same order of magnitude as that of the first overshoot if the enhancement took place in the lower resolution levels of the pyramid. This property accounts for the impression that in the enhanced images, artifacts occur only at a relatively large scale—they are always present, but become visible only in the enhancement of larger scales.

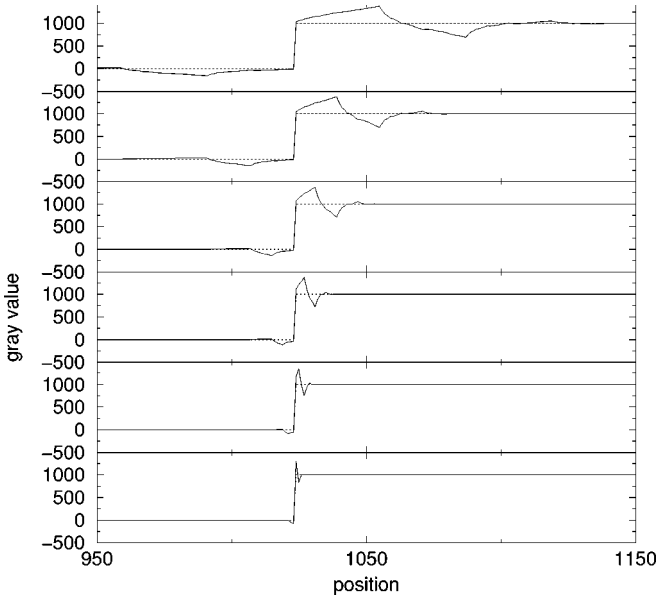

Fig. 13. Effect of linear enhancement of a single level (multiplication of the wavelet coefficients by a factor of two) for Daubechies 4th order wavelet. From bottom to top: result of enhancement of level 1, 2, …, 6. The dotted line shows the original edge.

The reason for the additional overshooting of the signal in the case of the FWT is the fact that the enhanced bandpass is high-pass filtered in the back-transform once more, thus emphasizing the edges even more. If no enhancement takes place, this effect cancels out when the signal is added to the corresponding low-pass, since the low-pass, too, was low-pass filtered once

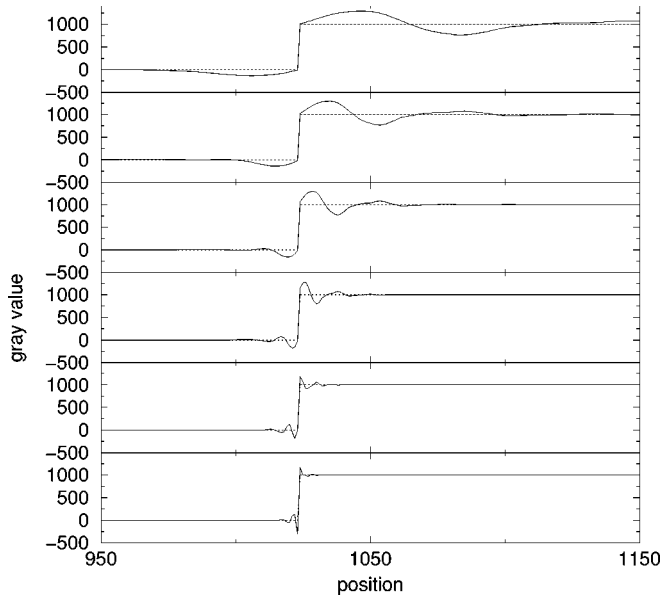

Fig. 14. Same as Fig. 13, but for a Daubechies 12th order wavelet.

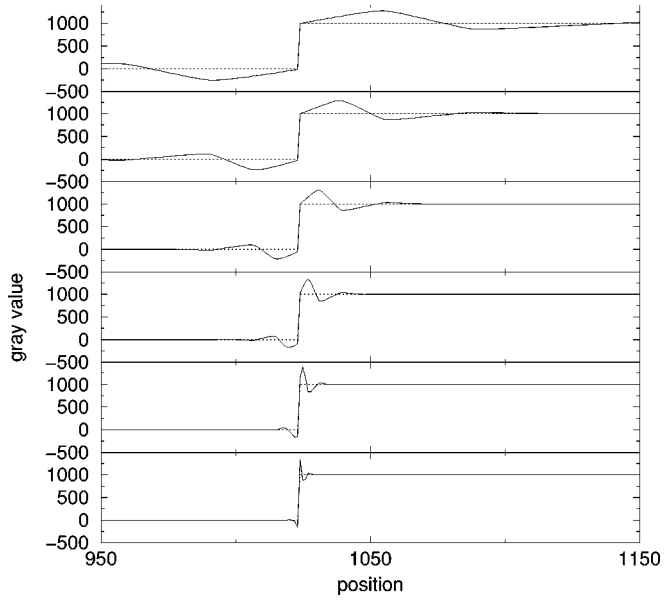

Fig. 15. Same as Fig. 13, but for the biorthogonal 7–9 tap wavelet.

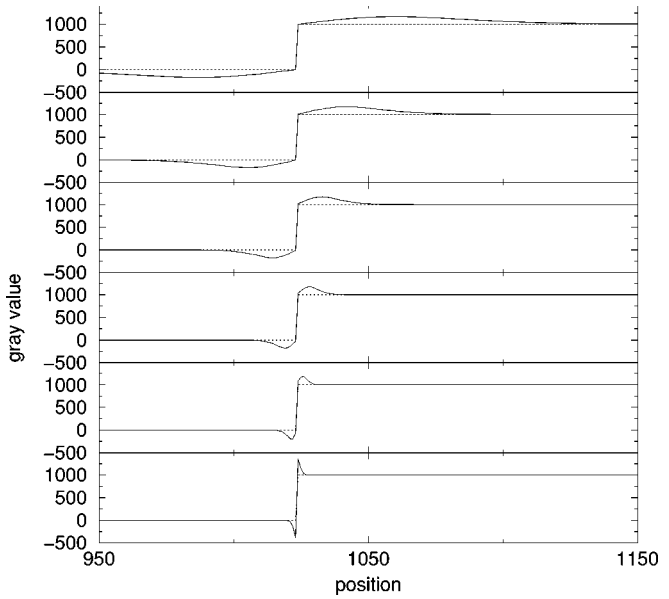

Fig. 16. Effect of linear enhancement of a single level (multiplication of the corresponding bandpass image by a factor of two) in the Laplacian Pyramid. From bottom to top: result of enhancement of level 1, 2, …, 6. The dotted line shows the original edge.

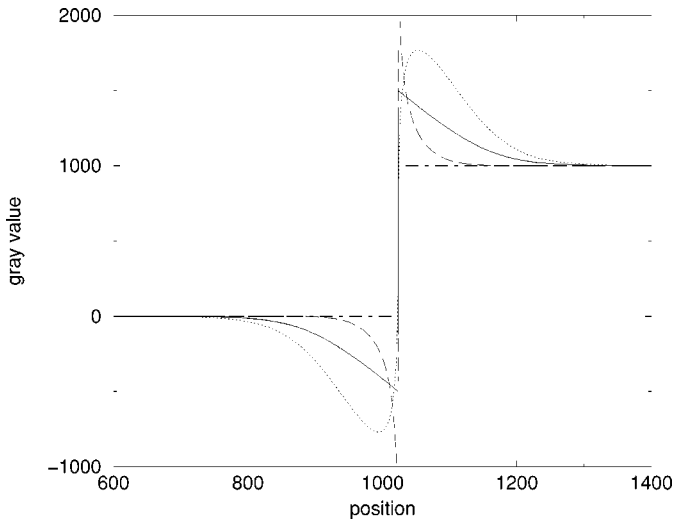

Fig. 17. Response of Laplacian Pyramid-based enhancement with varying gain to a step edge. The remapping function was linear. Dotted-dashed line: original edge; full line: $g_0 = \cdots = g_6 = 2.0$; long-dashed line: $g_0 = 4.0$, $g_1 = 3.5$, $g_2 = 3.0$, $g_3 = 2.5$, $g_4 = 2.0$, $g_5 = 1.5$, $g_6 = 1.0$; dotted line: $g_0 = 1.0$, $g_1 = 1.5$, $g_2 = 2.0$, $g_3 = 2.5$, $g_4 = 3.0$, $g_5 = 3.5$, $g_6 = 4.0$.

more in the back-transform. If, however, certain levels are enhanced, the effects do not cancel any more. In the Laplacian Pyramid, on the other hand, only smoothing operations take place in the back-transform, thus smearing out the edge enhancement particularly at lower scales.

The effect of the multiscale enhancement with varying gain becomes even clearer if we consider its response to a (sharp) step edge and to a softer edge (the step edge smoothed with a box kernel of size 150). The effect of both Laplacian Pyramid and FWT-based enhancement with varying gain for these kinds of edges is shown in Figs. 17–20.

Fig. 17 shows that in the Laplacian Pyramid, a pronouncement of the higher frequencies results in a very sharp accentuation of the edge, while a pronouncement of lower frequencies still enhances the edge, but far more softly and not by the same amplitude. Equal enhancement of all scales clearly has the same effect as unsharp masking with a correspondingly large kernel. For the FWT-based enhancement, results are similar (see Fig. 18), though again disturbed by a second overshoot. It should be noted, too, that even though the extension of the enhanced edge is similar in both cases (Laplacian Pyramid and FWT), it decays much faster in the beginning for the FWT, i.e., looks sharper.

For a soft edge, the difference between Laplacian Pyramid-based and wavelet-based enhancement is even more striking. Fig. 19 shows that in fact, since the edge only reaches a significant slope at the lower levels of the pyramid, equally strong enhancement of all scales leads to a very similar result as particularly strong enhancement on the lowest scale. For the FWT,

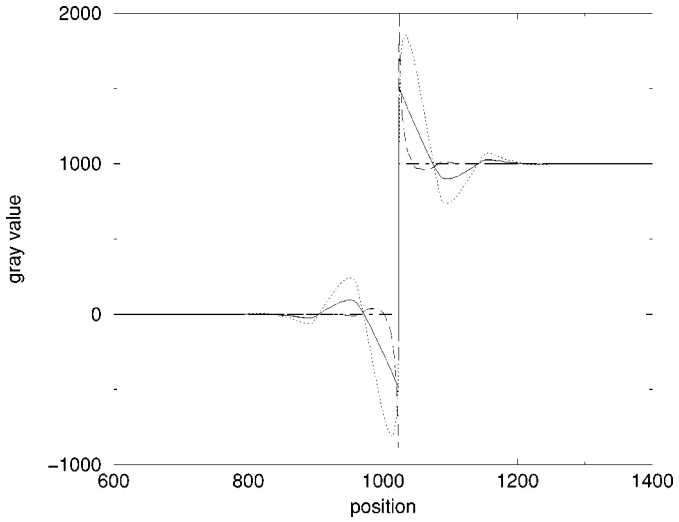

Fig. 18. Response of wavelet-based enhancement with varying gain to a step edge. Line styles are the same as in Fig. 17.

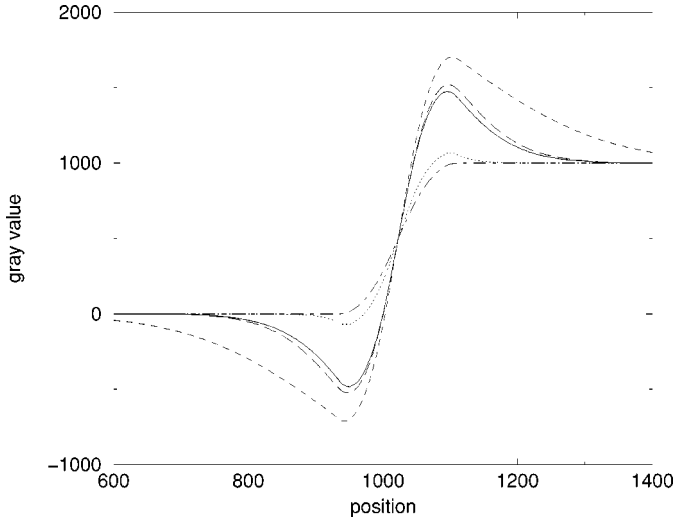

Fig. 19. Response of Laplacian Pyramid-based enhancement with varying gain to a soft edge. Line styles are the same as in Fig. 17. The dashed line additionally shows the result for equally strong enhancement in all levels, but for a Laplacian Pyramid with one more decomposition level.

the picture is completely different. Here, hardly any response to the enhancement is discernible in Fig. 20 if the same number of pyramid levels as before is used. The edge cannot be resolved in the same number of levels as within the Laplacian Pyramid framework. If we use one more level in the decomposition, the enhanced edge appears, though spoilt by the same artifacts as the sharp edge. The second overshoot is even more severe than for the sharp edge. Besides, even if we only take into account the first overshoot enhancing the edge, the amount of enhancement is less than in the case of the Laplacian Pyramid.

From the response shown in Figs. 17–20 it can be concluded that one may not achieve a similar image impression as for the Laplacian Pyramid by means of an enhancement via the FWT. Though remapping of the highest levels only would look very similar to the results of the Laplacian Pyramid (even might bring out fine structures better), there is no way in which a satisfactory (artifact-free) enhancement of larger structures might be

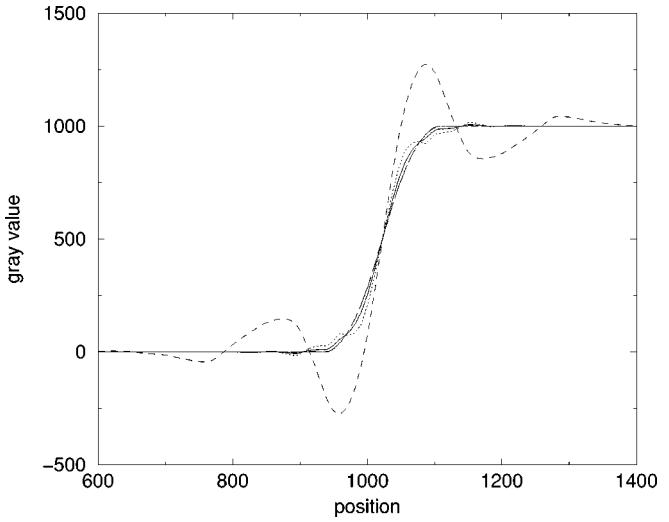

Fig. 20. Response of wavelet-based enhancement with varying gain to a soft edge. Line styles are the same as in Fig. 17. The dashed line additionally shows the result for equally strong enhancement in all levels, but for a FWT one level deeper.

achieved. Also, a nonlinear remapping function would not overcome this problem.

IV. Discussion

The results presented in the previous section show that although the FWT has some properties that seem to make it a good candidate for multiscale image enhancement (orthogonality of corresponding high- and low-pass, direction sensitivity, good sensitivity for small structures), there is a problem arising from the fact that in the back-transform, the high-pass has to be filtered with a wavelet once more before adding it to the corresponding low-pass, thus producing visible ringing artifacts if the corresponding high-pass was previously enhanced. In fact, this is not a completely new aspect—the artifacts that occur when different levels are enhanced differently lead to similar problems as too strong quantization in compression with wavelets [22]. Still, the problem is not so severe in compression applications, since best compression rates can be achieved particularly by compressing higher scales, which are not that sensitive to these artifacts. However, in the multiscale enhancement of images, we particularly want to explore the possibilities of enhancement of lower levels. However, since very small details seem to be enhanced better by the FWT than by the Laplacian Pyramid, in an enhancement based on the remapping of the higher levels only, the FWT might yield better results than the standard technique. Also, noise might be filtered out better by a wavelet transform.

The results presented previously by Laine *et al.* [13], [14] actually confirm our results. The enhanced images they produced with the redundant wavelet transform are very similar to ours which were enhanced with the Laplacian Pyramid. This is due to the fact that the filter used there is essentially a Laplacian and the back-transform filter in this case is a smoothing filter, just like in the Laplacian Pyramid. The enhancement results for other wavelet transform types shown in [13] alter the image impression so thoroughly, that they would be inappropriate for general radiographic applications.

A comparison of the images enhanced linearly and nonlinearly in the framework of a Laplacian Pyramid decomposition shows that nonlinearity of the remapping function is indeed an important feature to avoid ringing artifacts at very strong edges. The analysis of the response of the filter to a step-edge shows that enhancement of higher levels enhances mostly sharp edges and small details. On the other hand, enhancement of lower levels enhances all edges, but the sharp edges are enhanced very softly, thus, probably giving rise to the "soft" image impression of certain images as remarked in our clinical study. Small details, by contrast, will not be enhanced if only the lower pyramid levels are enhanced, since they are smoothed out there already.

V. Conclusion

We have shown that for the enhancement of radiographs in general, decomposition by an FWT leads to undesirable artifacts in the enhanced images. By contrast, the Laplacian Pyramid seems to be a more suitable decomposition method for multiscale enhancement, since it is free from such artifacts and results in very balanced image impression. The detailed discussion of other wavelet decomposition methods is beyond the scope of this paper, since here, we restrict ourselves to pyramidal implementations of the decomposition for reasons of time and space constraints in the processing chain of digital radiography system. However, as we have shown, in the case of a pyramidal decomposition of the image, the Laplacian Pyramid seems to be the method of choice.

Acknowledgment

The authors would like to thank T. Netsch and U. Mahlmeister for many discussions and helpful suggestions concerning this manuscript.

References

[1] A. R. Cowen, A. Giles, A. G. Davies, and A. Workman, "An image processing algorithm for PPCR imaging," in *Proc. SPIE Image Processing*, vol. 1898, 1993, pp. 833–843.

[2] W. Qian, L. P. Clarke, and B. Zheng, "Computer assisted diagnosis for digital mammography," *IEEE Eng. Med. Biol. Mag.*, vol. 14, pp. 561–569, Sept./Oct. 1995.

[3] M. Unser, P. Thévenaz, C. Lee, and U. E. Ruttiman, "Registration and statistical analysis of pet images," *IEEE Eng. Med. Biol. Mag.*, vol. 14, pp. 603–611, Sept./Oct. 1995.

[4] J. B. Weaver, X. Yansun Jr., D. M. Healy, and L. D. Cromwell, "Filtering noise from images with wavelet transforms," *Magn. Reson. Med.*, vol. 21, no. 2, pp. 288–295, 1991.

[5] P. Saipetch, B. K. T. Ho, R. Panwar, M. Ma, and J. Wei, "Applying wavelet transforms with arithmetic coding to radiological image compression," *IEEE Eng. Med. Biol. Mag.*, vol. 14, pp. 587–593, Sept./Oct. 1995.

[6] A. Manduca, "Compressing images with wavelet/subband coding," *IEEE Eng. Med. Biol. Mag.*, vol. 14, pp. 639–646, Sept./Oct. 1995.

[7] Z. Yang, M. Kallergi, R. A. DeVore, B. Lucier, W. Qian, R. A. Clark, and L. P. Clarke, "Effect of wavelet bases on compressing digital mammograms," *IEEE Eng. Med. Biol. Mag.*, vol. 14, pp. 570–577, Sept./Oct. 1995.

[8] M. Unser and A. Aldroubi, "A review of wavelets in biomedical applications," *Proc. IEEE*, vol. 84, pp. 626–638, Apr. 1996.

[9] P. Vuylsteke and E. Schoeters, "Multiscale image contrast amplification (MUSICA™)," in *Proc. SPIE Image Processing*, vol. 2167, 1994, pp. 551–560.

[10] M. Stahl, T. Aach, T. M. Buzug, S. Dippel, and U. Neitzel, "Noise-resistant weak-structure enhancement for digital radiography," in *Proc. SPIE Med. Imag.*, 1999, vol. 3661, pp. 1406–1417.

[11] E. Dencker, M. Stahl, S. Dippel, C. M. Schaefer-Prokop, S. Baus, S. Goehde, D. Hoegemann, A. Leppert, and M. Galanski, "Nonlinear multiscale processing in selenium-based chest radiography," in *ECR, Book of Abstracts*. Vienna, Austria: ECR, 1999.

[12] J. Lu, D. M. Healy, and J. B. Weaver, "Contrast enhancement of medical images using multiscale edge representation," *Opt. Eng.*, vol. 33, no. 7, pp. 2151–2161, 1994.

[13] A. Laine, J. Fan, and W. Yang, "Wavelets for contrast enhancement of digital mammography," *IEEE Eng. Med. Biol. Mag.*, vol. 14, pp. 536–550, Sept./Oct. 1995.

[14] X. Zong, A. F. Laine, E. A. Geiser, and D. C. Wilson, "De-noising and contrast enhancement via wavelet shrinkage and nonlinear adaptive gain," in *Proc. SPIE Wavelet Applications III*, vol. 2762, 1996, pp. 566–574.

[15] J.-P. Bolet, A. R. Cowen, J. Launders, A. G. Davies, G. J. S. Parkin, and R. F. Bury, "Progress with an "all-wavelet" approach to image enhancement and de-noising of direct digital thorax radiographic images," in *Proc. 6th Int. Conf. Image Processing and its Applications*, vol. 1, Dublin, Ireland, 1997, Conf. Publ. 443, pp. 244–248.

[16] P. J. Burt and E. H. Adelson, "The Laplacian pyramid as a compact image code," *IEEE Trans. Commun.*, vol. COMM–31, pp. 532–540, Apr. 1983.

[17] S. G. Mallat, "Multifrequency channel decompositions of images and wavelet models," *IEEE Trans. Acoust. Speech Signal. Processing*, vol. 37, pp. 2091–2110, Dec. 1989.

[18] ——, "A theory for multiresolution signal decomposition: The wavelet representation," *IEEE Trans. Pattern. Anal. Machine Intell.*, vol. 11, pp. 674–693, July 1989.

[19] M. Antonini, M. Barlaud, P. Mathieu, and I. Daubechies, "Image coding using wavelet transforms," *IEEE Trans. Image Processing*, vol. 1, pp. 205–220, Mar. 1992.

[20] S. Mallat and S. Zhong, "Characterization of signals from multiscale edges," *IEEE Trans. Pattern Anal. Machine Intell.*, vol. 14, pp. 710–732, July 1992.

[21] I. Daubechies, *Ten Lectures on Wavelets*. Philadelphia, PA: SIAM, 1992.

[22] G. Strang and T. Nguyen, *Wavelets and Filter Banks*. Wellesley, MA: Wellesley-Cambridge Press, 1996.

[23] M. Stahl, T. Aach, and S. Dippel, "Digital radiography enhancement by nonlinear multiscale processing," *Med. Phys.*, vol. 27, no. 1, pp. 56–65, 2000.